International Symposium
On Turbulence and Shear Flow
Phenomena (TSFP-8)
August 28 - 30, 2013 Poitiers, France

A NOVEL DYNAMIC FORCING SCHEME INCORPORATING BACKSCATTER FOR HYBRID RANS/LES

Qian-Qiu Xun and Bing-Chen Wang
Dept. of Mechanical & Manufacturing Engineering
Univ. of Manitoba
Winnipeg, MB, R3T 5V6, Canada
umxunq@cc.umanitoba.ca, BingChen.Wang@ad.umanitoba.ca

ABSTRACT

In this paper, we present a novel dynamic forcing scheme incorporating backscatter in order to remove the artificial buffer layer in the hybrid RANS/LES approach. In contrast to previous forcing techniques, the proposed forcing scheme is determined dynamically from the flow field itself, and does not require any extraction of turbulent fields from reference databases obtained using direct numerical simulation (DNS) or wall-resolved LES. Transport equations for the resolved stresses and turbulent kinetic energy are introduced to investigate the effects of dynamic forcing on reduction of the thickness of the artificial buffer layer. The proposed forcing model has been tested in the context of turbulent channel flows with Reynolds numbers $Re_\tau = 650$ and 1020. In order to validate the hybrid RANS/LES approach, the first- and second-order flow statistics obtained are thoroughly compared with the available DNS data.

INTRODUCTION

In large-eddy simulation (LES), a flow field is typically decomposed into resolved large scale components and unresolved subgrid-scale (SGS) components through a filtering process. Application of LES to wall-bounded flows at high Reynolds numbers represents a challenge in the area of the computational fluid dynamics. The presence of a solid boundary creates significant difficulty for LES to resolve the wall shear layer and capture the important energy-producing events in the near-wall region. This is because as the wall is approached, viscous forces become dominant, and the computational resources needed for resolving the viscous scales increases exponentially. Chapman (1979) estimated that the number of grid points is proportional to $Re_\ell^{1.8}$ (based on an integral length scale ℓ) for LES to resolve the wall shear layer.

In order to alleviate the very fine resolution required for the wall shear layer, hybrid RANS/LES approach was introduced by Spalart *et al.* (1997). In hybrid RANS/LES, the Reynolds-averaged Navier-Stokes (RANS) method is used to treat the near-wall region and LES is applied to the core turbulent region. Owing to the incompatibility of these two numerical modelling approaches, an artificial (i.e., non-physical) buffer layer forms along the interface where the closure model switches from RANS to LES. The effect of the artificial buffer layer (Nikitin *et al.*, 2000) can be identified in the simulation of a plane channel flow, where the mean streamwise velocity profile shifts apparently from the log-law. Baggett (1998) performed their hybrid simulations using $\overline{v^2}$-f RANS model (where $\overline{v^2}$ and f denote the velocity scalar associated with velocity fluctuations and the elliptic relaxation factor, respectively) of Durbin (1995) in the near-wall region. He observed non-physical streak-like structures in the RANS zone. These 'super-streaks' have spanwise lengths over approximately of two grid points, and overly large streamwise lengths. He further indicated that these 'super-streaks' cause a de-correlation of the streamwise and wall-normal velocity components.

The artificial buffer layer is a rather robust feature of hybrid RANS/LES, with little dependence upon the details of the specific closure models, interface locations, matching conditions, and grid resolutions. Many studies (Nikitin *et al.*, 2000; Temmerman *et al.*, 2005; Piomelli *et al.*, 2003; Davidson & Dahlström, 2005) have been conducted to test the locations of the modelling interface, all resulting in similar velocity shift. It has been solidly proven that the velocity shift is an intrinsic character to hybrid RANS/LES, which cannot be removed by simply using different matching conditions (Tucker & Davidson, 2004) and different turbulence closure models (Nikitin *et al.*, 2000; Tucker & Davidson, 2004; Temmerman *et al.*, 2005). Furthermore, tests on grid refinements have shown that even after the solution reaches a grid independent state there still exists a velocity shift (Larsson *et al.*, 2007).

Several strategies have been proposed to remove the artificial buffer layer through additional forcing in the momentum equations. The forcing can be either obtained from a stochastic model, or extracted from a reference DNS or wall resolved LES databases of a fully developed channel flow. Piomelli *et al.* (2003) used forcing to account for backscatter, and suggested that it should have length and time scales on the order of the grid size and time step, respectively. Their forcing field consisted of essentially white noises, and with which, they were able to lower down the velocity shift and had the super-streaks broken up. Batten *et al.* (2004) and Davidson & Billson (2006) proposed stochastic models that generate forcing fields with predefined spectra and anisotropy. They observed quicker transition from modelled turbulence in RANS to resolved turbulence in LES and a desirable reduced artificial buffer layer. Davidson & Dahlström (2005) and Larsson *et al.* (2007) extracted the forcing field from a reference database (DNS or wall-resolved LES) in order to make the forcing field realistic in flow physics (to be compatible with, e.g. coherent

structures). With this technique, they were able to obtain a lower velocity shift, a smaller artificial buffer layer and reduced near-wall super-streaks.

Notwithstanding the achievements mentioned above, lack of physical justification due to use of stochastic models, and a need of in-hand database for extraction of forcing schemes prevent in-depth understanding of the physics underlying the formation of the artificial buffer layer. In contrast to the previous approaches, in this paper, we aim to propose an interesting physics-based dynamic forcing scheme using backscatter obtained from the flow field itself. Furthermore, the effects of dynamic forcing on reducing the thickness and impact of the artificial buffer layer will be analyzed, which identifies the important factors for improving the forcing techniques.

CLOSURE MODELS AND THE DYNAMIC FORCING SCHEME

In hybrid RANS/LES, the spatially filtered continuity and momentum equations take the following form for an incompressible flow:

$$\frac{\partial \bar{u}_i}{\partial x_i} = 0 \tag{1}$$

$$\frac{\partial \bar{u}_i}{\partial t} + \frac{\partial}{\partial x_j}(\bar{u}_i \bar{u}_j) = -\frac{1}{\rho}\frac{\partial \bar{p}}{\partial x_i} + \frac{u_\tau^2}{\delta}\delta_{1i} + \frac{\partial}{\partial x_j}\left[(\nu + \nu_t)\frac{\partial \bar{u}_i}{\partial x_j}\right] + f_i \tag{2}$$

where $\bar{p}$ represents the effective pressure combined with the isotropic part of the Reynolds stress tensor for RANS or SGS stress tensor for LES, $(u_\tau^2/\delta)\delta_{1i}$ is the imposed constant mean pressure gradient along the streamwise direction, δ_{ij} is the Kronecker delta, and δ is the half channel height (see Fig. 1). As a consequence of the filtering or averaging process, the so-called eddy viscosity ν_t appear in the above system of governing equations. In this paper, we use ν_t^R and ν_t^L to distinguish the eddy viscosity for RANS and LES, respectively.

Nikitin *et al.* (2000), Temmerman *et al.* (2005) and Davidson & Dahlström (2005) have obtained qualitatively similar results using a variety of eddy viscosity turbulence closure models in the context of hybrid RANS/LES. Based on their observations, in this paper, we use simple algebraic models for closure of the governing equations, and focus our attention on testing a novel forcing scheme to tackle directly the challenges from the velocity shift and artificial buffer layer. In the inner layer, the mixing length model with wall damping function is used. In the outer layer, the Smagorinsky model (Smagorinsky, 1963) is used, and the value of the Smagorinsky coefficient is fixed to $C_S = 0.0042$ in current hybrid RANS/LES simulations in this paper.

In order to match the values of ν_t^R and ν_t^L at the interface of the RANS and LES zones, Nikitin *et al.* (2000) and Temmerman *et al.* (2005) enforced continuity of ν_t, whereas Baggett (1998) and Larsson *et al.* (2007) used blending functions. However, the results of these researchers are similar to those of Davidson & Peng (2003), whose hybrid approach is free from any special treatment for ν_t. Because the exact matching conditions appear to have a marginal effect on the appearance of an artificial buffer layer, we follow the approach of Davidson & Peng (2003) and ν_t is neither enforced nor blended in the current research.

The forcing term f_i in Eq. (2) is defined as:

$$f_i = -\frac{\partial \tau_{ij}^B}{\partial x_j} \tag{3}$$

where τ_{ij}^B denotes the stress tensor which can account for backscatter in our proposed modelling approach. In order to implement a forcing scheme in a hybrid RANS/LES approach, it is essential to understand at which length scale the forcing should be applied. Since backscatter is a direct result of the interactions between the resolved and subgrid scale motions, the length scale is chosen to be the grid level filter width, which overlaps the nodal distance of the grid system in a conventional LES approach. The stress tensor τ_{ij}^B stems from the dynamic nonlinear model of Wang & Bergstrom (2005) and takes the following form:

$$\tau_{ij}^B = -C_W \gamma_{ij} - C_N \eta_{ij} \tag{4}$$

where γ_{ij} and η_{ij} represent two quadratic base tensor functions defined as $\gamma_{ij} \overset{\text{def}}{=} 4\bar{\Delta}^2(\bar{S}_{ik}\bar{\Omega}_{kj} + \bar{S}_{jk}\bar{\Omega}_{ki})$ and $\eta_{ij} \overset{\text{def}}{=} 4\bar{\Delta}^2(\bar{S}_{ik}\bar{S}_{kj} - \bar{S}_{mn}\bar{S}_{nm}\delta_{ij}/3)$, respectively; and $\bar{\Delta}$ is the grid-level filter size, $\bar{S}_{ij} \overset{\text{def}}{=} (\partial\bar{u}_i/\partial x_j + \partial\bar{u}_j/\partial x_i)/2$ is the resolved strain rate tensor, and $\bar{\Omega}_{ij} \overset{\text{def}}{=} (\partial\bar{u}_i/\partial x_j - \partial\bar{u}_j/\partial x_i)/2$ is the resolved rotation rate tensor.

Coefficients C_W and C_N in the forcing scheme (cf. Eq. (4)) are computed dynamically at each time step (Germano *et al.*, 1991; Lilly, 1992) and their values are self-adjusted in accordance with the instantaneous flow field. Following Piomelli *et al.* (2003), who used the filter width and time step as the spatial and temporal scales in their stochastic forcing model, the characteristic time scale at which the present forcing scheme is applied overlaps the simulation time step. The first term γ_{ij} does not make any contribution to the kinetic energy (KE) transfer between the resolved and subgrid scales, but according to a recent systematic *a priori* LES study of Horiuti (2003), it significantly improves the correlation between the exact SGS stress extracted from a DNS database and that predicted by LES. As demonstrated in previously full LES studies (Wang & Bergstrom, 2005), it is the second term η_{ij} that contributes significantly to the backscatter of KE from the subgrid to the resolved scales.

TEST CASE AND NUMERICAL ALGORITHM

Fig. 1 shows the computational domain of the plane channel and coordinate system used in the hybrid approach. The dimensions of the computational domain are $L_1 \times L_2 \times L_3 = 2.5\pi\delta \times 2\delta \times \pi\delta$ in the streamwise (x_1), wall-normal (x_2) and spanwise (x_3) directions, respectively. Two Reynolds numbers have been tested in this study, i.e. $Re_\tau \overset{\text{def}}{=} u_\tau\delta/\nu = 650$ and 1020. The grid is uniform in the streamwise and spanwise directions, and stretched in the wall-normal direction using a hyperbolic-tangent function in order to provide a greater resolution in the near-wall region.

A finite volume method based on a collocated grid system was applied to the discretization of the governing equations. Following the approach of Choi & Moin (1994), the filtered momentum equations were solved using a fractional-step method. The nonlinear term was discretized using a second-order explicit Adams-Bashforth

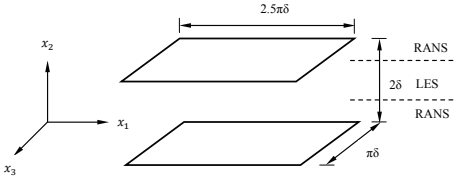

Figure 1. Computational domain for hybrid RANS/LES of a channel flow.

scheme and the viscous diffusion term was discretized using a second-order Crank-Nicolson scheme. A second-order central difference scheme was applied for the spatial discretization as it represents a good compromise between accuracy, simplicity and efficiency (Ferziger & Perić, 1999). The Poisson type pressure equation derived from the continuity equation was solved using a multi-grid method.

No slip and impermeable boundary conditions are imposed on the velocity components at the walls. Periodic boundary conditions are employed in the streamwise and spanwise directions since the flow field is assumed to be statistically homogeneous in these two directions. Statistics of various flow variables are calculated after the fluid field has become turbulent and fully developed. In the presentation of the results, quantities non-dimensionalized using the friction velocity $u_\tau \overset{\text{def}}{=} \sqrt{\tau_w/\rho}$ (where τ_w represents the wall shear stress) are denoted with a superscript '+'.

NUMERICAL RESULTS

In this section, flow statistics obtained from hybrid RANS/LES will be thoroughly analyzed, which include the resolved mean velocity, resolved velocity fluctuations, resolved turbulent shear stresses and TKE, backward scatter of KE from the subgrid to resolved scales, and budget of total shear stresses. Furthermore, the physics underlying the formation of the artificial buffer layer will be studied, and the effects of the proposed forcing term on breaking-up of super-streaks and on reduction of the velocity shift and artificial buffer layer will be discussed.

An instantaneous filtered quantity $\bar{\phi}$ can be decomposed into a time- and plane-averaged component and a residual component as: $\bar{\phi} = \langle\bar{\phi}\rangle + \bar{\phi}''$.

Then the predicted resolved velocity fluctuations (or root-mean-square (RMS) values) can be defined as

$$\bar{u}^+_{i,\text{rms}} \overset{\text{def}}{=} \left\langle \left(\frac{\bar{u}_i - \langle\bar{u}_i\rangle}{u_\tau} \right)^2 \right\rangle^{1/2} = \frac{\langle \bar{u}_i''^2 \rangle^{1/2}}{u_\tau} \tag{5}$$

for $i = 1$, 2 and 3 respectively.

The physics underlying the formation of the artificial buffer layer, and the effects of the dynamic forcing on reducing the thickness and impact of the artificial buffer layer, can be well interpreted by utilizing transport equations for the resolved turbulent stresses. These transport equations have been derived and documented in the full LES study of Xun *et al.* (2011) on a rotating turbulent channel flow. It is worthwhile to note that the production terms in the transport equations have a significant influence on the absolute value and distribution of the resolved turbulent shear stresses (i.e., $-\langle\bar{u}_i''\bar{u}_j''\rangle$) and TKE (i.e., $\frac{1}{2}\langle\bar{u}_i''\bar{u}_i''\rangle$). The production term for the resolved shear stress component $-\langle\bar{u}_1''\bar{u}_2''\rangle$ in a fully developed turbulent channel flow is given by

$$\langle P_{12}\rangle = \langle \bar{u}_2''^2 \rangle \frac{d\langle\bar{u}_1\rangle}{dx_2} \tag{6}$$

and those for the resolved normal stress components $\langle\bar{u}_j''\bar{u}_j''\rangle$ (no summation implied here) are given by

$$\langle P_{11}\rangle = -2\langle\bar{u}_1''\bar{u}_2''\rangle \frac{d\langle\bar{u}_1\rangle}{dx_2} \tag{7}$$

$$\langle P_{22}\rangle = 0 \tag{8}$$

$$\langle P_{33}\rangle = 0 \tag{9}$$

The production term for the resolved TKE can be obtained by taking one half of the sum of Eqs. (7)-(9), i.e.

$$\langle P_k\rangle = -\langle\bar{u}_1''\bar{u}_2''\rangle \frac{d\langle\bar{u}_1\rangle}{dx_2} \tag{10}$$

The term on the right-hand-side (RHS) of Eqs. (6)–(10) implies the production arising from the mean resolved turbulent (shear and normal) stresses. In a fully developed channel flow, $-\langle\bar{u}_1''\bar{u}_2''\rangle$ has the same parity as $d\langle\bar{u}_1\rangle/dx_2$, both of which are positive and negative for $x_2 < 0$ and $x_2 > 0$, respectively. As a result, $P_{11} > 0$ holds across the entire channel, whereas P_{12} assumes a sign that is opposite to that of x_2. Because $P_{22} = P_{33} = 0$, there is no direct production for either $\langle\bar{u}_2''^2\rangle$ or $\langle\bar{u}_3''^2\rangle$ from the resolved turbulent stresses. Nevertheless, energy redistributes within the system and influences both these terms through the mechanisms of molecular diffusion, SGS production and diffusion, and pressure-strain interactions (Xun *et al.*, 2011).

In order to validate the proposed dynamic forcing scheme for hybrid RANS/LES, the numerical results obtained at two Reynolds numbers are compared with two sets of DNS data obtained by Abe *et al.* (2004) (designated as AKM-2004, $Re_\tau = 1020$) and Iwamoto *et al.* (2002) (designated as ISK-2002, $Re_\tau = 650$), respectively. Furthermore, in order to demonstrate the advantages of the proposed method, in the next two subsections, the results on hybrid RANS/LES with and without forcing will be compared.

Hybrid RANS/LES without Forcing

As shown in Fig. 2(a), for hybrid RANS/LES without forcing, the mean velocity profile deviates significantly from the profile of the familiar log-law, and it is apparent that there exists a velocity shift. This incorrect prediction of the mean velocity profile by hybrid RANS/LES without forcing is a classical pattern, which has been observed in many previous studies. The discrepancy between the predicted mean velocity profile and the standard log-law is due to the existence of the artificial buffer layer between the LES zone and RANS zone. Baggett (1998) found the presence of very elongated non-physical 'super-streaks' in his hybrid RANS/LES study of a turbulent plane channel flow. These super-streaks cause a de-correlation between streamwise and wall-normal fluctuations. The observation of Baggett (1998) is confirmed by the current study. As clearly shown in Fig. 3, super-streaks exist in the current flow (obtained using hybrid RANS/LES without forcing) and can be effectively demonstrated using the isopleths of instantaneous streamwise velocity fluctuations in the x_1-x_3 plane at the interface $x^+_{2,\text{interface}} = 39$.

The formation of the artificial buffer layer (indicated by larger gradient of the resolved mean velocity around the interface) can be well explained by utilizing transport equations of turbulent stresses. Because of the de-correlation between streamwise and wall-normal fluctuations, the redistribution of energy from the streamwise to the wall-normal

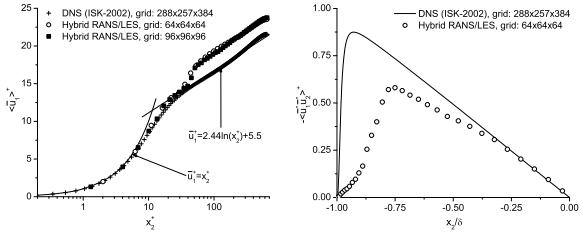

(a) Resolved mean velocity (b) Resolved shear stress

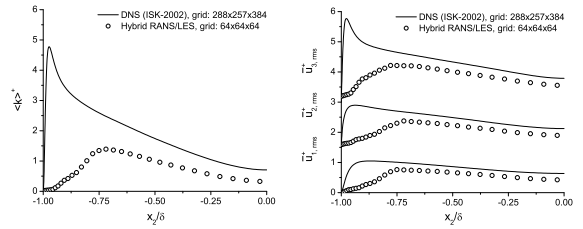

(c) Resolved TKE (d) Resolved RMS velocities

Figure 2. Flow statistics for hybrid RANS/LES without forcing ($Re_\tau = 650$; interface: $x^+_{2,\,\text{interface}} = 39$). (d) Offset for clarity, from top to bottom: $\bar{u}^+_{1,\,\text{rms}}$, $\bar{u}^+_{3,\,\text{rms}}$ and $\bar{u}^+_{2,\,\text{rms}}$.

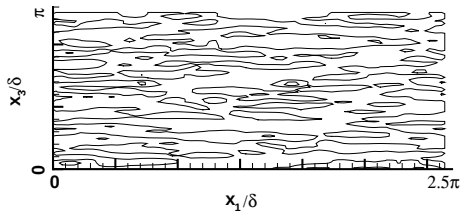

Figure 3. Isopleths of instantaneous streamwise velocity fluctuations in x_1-x_3 plane at interface $x^+_{2,\,\text{interface}} = 39$ for hybrid RANS/LES without forcing ($Re_\tau = 650$; grid: $64 \times 64 \times 64$).

component is suppressed. This is evident that $\bar{u}_{2,\text{rms}}$ is excessively damped around the interface in Fig. 2(d). Consequently, the velocity must shift upwards from the standard log-law (exhibiting an overly large gradient) in order to compensate the production P_{12} for the resolved shear stress (cf. Eq. (6)). However, as shown in Fig. 2(b), the level of the resolved shear stress $-\langle \bar{u}_1'' \bar{u}_2'' \rangle$ is much reduced, which then leads to decreases in the values of the production terms P_k and P_{11}. This inevitably results in unreasonably low levels of resolved TKE and $\bar{u}_{1,\text{rms}}$ (see Eqs. (7) and (10)), which is clearly shown in Figs. 2(c) and 2(d), respectively.

Hybrid RANS/LES with Dynamic Forcing

The SGS dissipation rate represents local KE transferred between the resolved and unresolved (subgrid) scales through an inertial and inviscid process. It represents the rate of KE production and functions as a source of KE for the residual SGS motions and a sink of KE for the large resolved scale motions. The instantaneous value of the SGS dissipation rate can be either positive or negative, representing a local forward or backward transfer of KE between the resolved and subgrid scales, respectively.

The proposed dynamic forcing scheme is associated with the following production term: $P^B_r = -\tau^B_{ij}\bar{S}_{ij}$.

Substituting the constitutive relation for the forcing scheme represented by Eq. (4), the following equation is

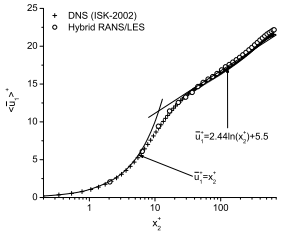

(a) Forcing in entire domain

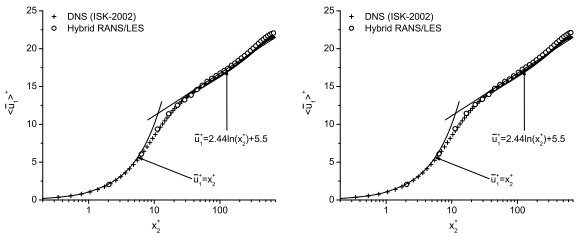

(b) Forcing in RANS zone (c) Forcing in LES zone

Figure 4. Resolved mean velocity profile obtained from hybrid RANS/LES with forcing applied to different regions ($Re_\tau = 650$; grid: $64 \times 64 \times 64$; interface: $x^+_{2,\,\text{interface}} = 39$).

obtained for evaluating P^B_r:

$$P^B_r = C_W \gamma_{ij} \bar{S}_{ij} + C_N \eta_{ij} \bar{S}_{ij} \tag{11}$$

According to Wang & Bergstrom (2005), in the above equation, the second term (i.e., $C_N \eta_{ij} \bar{S}_{ij}$) plays a pivotal role in the local KE backscatter, however the first term is zero (i.e., $C_W \gamma_{ij} \bar{S}_{ij} \equiv 0$) because γ_{ij} is anti-symmetrical tensor and $\bar{S}_{ij}$ is a symmetrical tensor.

To date, the forcing techniques using backscatter have been applied exclusively in either the RANS zone or the LES zone in previous hybrid RANS/LES studies. One may expect small scale flow motions are potentially effective in breaking up super-streaks, and therefore, the forcing should be applied to the RANS region. However, one could also argue that the forcing should be applied to the large scales which carry most of TKE and are responsible for generating Reynolds stresses in the LES zone. The debate on this issue has not been concluded in literature. Piomelli *et al.* (2003) employed backscatter forcing in the RANS region below the interface, however, Davidson (2009) added backscatter forcing to special scales in the LES region for $x^+_{2,\text{interface}} < x^+_2 < 2x^+_{2,\text{interface}}$. In this paper, in order to investigate the effects of forcing region on the predictive accuracy of the hybrid approach, we test our present backscatter forcing in three different region: (1) in entire domain ($0 < x^+_2 < \delta^+$), (2) in RANS region only ($0 < x^+_2 < x^+_{2,\text{interface}}$), and (3) in LES region only ($x^+_{2,\text{interface}} < x^+_2 < \delta^+$). As shown in Figs. 4(a)–(c), the artificial buffer layer has been successfully removed for all three cases regardless the choices of the forcing region.

Figs. 5(a)–(c) show the time- and plane-averaged profile of P^B_r for the three forcing regions tested. The value of $\langle P^B_r \rangle$ has been non-dimensionalized using u^4_τ/ν, which is negative across the entire channel, representing a net effect of backscatter. Although the resolved mean velocity profiles (outputs) obtained using different forcing regions are very similar in Fig. 4, the backscatter (input) itself shows distinctively different patterns. As shown in Fig. 5(a), when forcing is applied across the entire channel, the magnitude

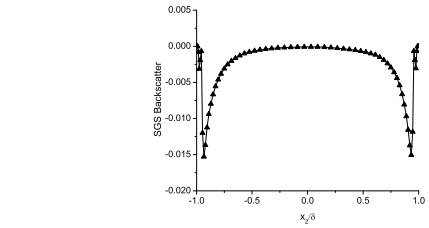

(a) Forcing in entire domain

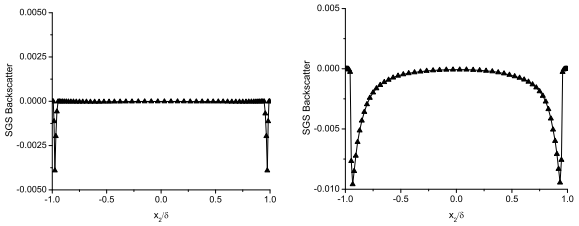

(b) Forcing in RANS zone (c) Forcing in LES zone

Figure 5. Time- and plane-averaged SGS KE backscatter predicted by hybrid RANS/LES with forcing applied to three different regions (non-dimensionalized using u_τ^4/ν; $Re_\tau = 650$; grid: $64 \times 64 \times 64$; interface: $x^+_{2,\,\text{interface}} = 39$).

of backscatter peaks right above the modelling interface location, then gradually decreases to zero as the core region is approached. There is a secondary peak for backscatter between the solid wall and the modelling interface. In Fig. 5(b), the magnitude of backscatter reaches its maximum between the solid wall and the modelling interface, then drastically goes to zero immediately outside of the interface (within the core region of the channel). This feature is expected, because the forcing is exclusively applied to RANS region. However, as shown in Fig. 5(c), when the forcing is applied in the LES region only, the magnitude of backscatter increases drastically from zero near the solid wall (i.e., in the RANS region) to its peak value right above the interface, and then gradually decreases back to zero in the core of the channel. The backscatter of KE (with a peak value in the RANS region as shown in Fig. 5(b) or immediately above the interface in the LES region shown in Figs. 5(a) and (c)) plays an important role in breaking up super-streaks and maintaining the proper level of turbulent shear stresses in the core region of the channel. This is also the key physical feature that contributes directly to reduction in the thickness of the artificial buffer layer and removal of the tenacious velocity shift pattern. Furthermore, it should be indicated that it is very desirable to observe that the value of the magnitude of $\langle P_r^B \rangle$ approaches zero automatically in the core turbulent region of the channel, which satisfies the physical requirement that the forcing should not affect the accurate LES predictions. Fig. 5 shows clear evidence that backscatter can be generated to properly treat the interfacing problem once the proposed forcing scheme is activated in either the RANS or the LES zone. This is an encouraging result, which is fundamental for stable and flexible numerical applications.

In comparison with Fig. 3, when forcing was added to different regions, smaller scales are indeed formed and the super-streaks are broken up at the interface $x^+_{2,\text{interface}} = 39$, which is evident in Figs. 6(a)–(c). This is consistent with the results that the velocity shift has been removed regardless the choices of the forcing region (see Fig. 4).

The proposed dynamic forcing scheme has also been

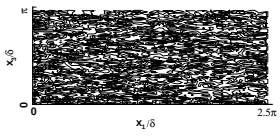

(a) Forcing in entire domain

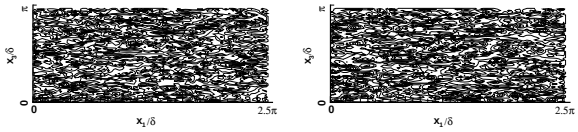

(b) Forcing in RANS zone (c) Forcing in LES zone

Figure 6. Isopleths of instantaneous streamwise velocity fluctuations in x_1-x_3 plane at interface $x^+_{2,\,\text{interface}} = 39$ with forcing applied to three different regions ($Re_\tau = 650$; grid: $64 \times 64 \times 64$).

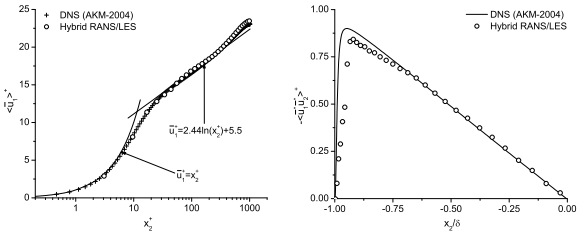

(a) Resolved mean velocity (b) Resolved shear stress

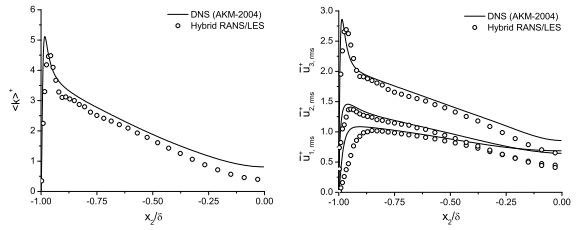

(c) Resolved TKE (d) Resolved RMS velocities

Figure 7. Flow statistics with forcing applied to the entire computational domain for $0 < x_2^+ < \delta^+$ ($Re_\tau = 1020$; grid: $96 \times 64 \times 64$; interface: $x^+_{2,\,\text{interface}} = 61$). (d) Offset for clarity, from top to bottom: $\bar{u}^+_{1,\,\text{rms}}$, $\bar{u}^+_{3,\,\text{rms}}$ and $\bar{u}^+_{2,\,\text{rms}}$.

tested at a higher Reynolds number $Re_\tau = 1020$. The resolved mean velocity profile is in excellent agreement with the DNS data of Abe *et al.* (2004) as shown in Fig. 7(a). Fig. 7(b) compares the time- and plane-averaged resolved turbulent shear stress obtained from the hybrid approach with 'true' Reynolds shear stress from the DNS approach. As shown in Figs. 7(c) and 7(d), in general, the trends predicted by hybrid RANS/LES are in agreement with DNS data. However, small differences are observed: the hybrid method either slightly overpredicts or slightly underpredicts the resolved TKE and RMS velocity in comparison with DNS data, depending on the region of the flow. Fig. 7 clearly demonstrates that the artificial buffer layer has been removed for the turbulent channel flow at $Re_\tau = 1020$, and hybrid RANS/LES is in general successful in reproducing the first- and second-order flow statistics.

Conclusions

In this paper, a novel dynamic forcing scheme incorporating backscatter is proposed for hybrid RANS/LES. The forcing is obtained from the flow field itself. Therefore, it

is more physically sound than the forcing based on stochastic white noises, and more convenient to implement than that extracted from reference DNS or wall resolved LES databases. It is demonstrated in this paper that backscatter can be generated to properly treat the interfacing problem once the proposed forcing scheme is activated in either the RANS or the LES zone. This is an encouraging modelling feature, which is fundamental for stable and flexible numerical applications.

In order to remove the artificial buffer layer, the conventional strategy has focused primarily on the eddy viscosity ν_t using approaches by, e.g. adjusting ν_t to an 'ideal' value to maintain the budget of shear stresses (Nikitin *et al.*, 2000; Mason & Thomson, 1992), and merging ν_t^R and ν_t^L using blending functions or different interface conditions (Temmerman *et al.*, 2005; Baggett, 1998). In contrast, the current hybrid approach, based on the dynamic forcing scheme incorporating backscatter, generates a proper level of $\bar{u}_{2,\mathrm{rms}}$ and $-\langle\bar{u}_1''\bar{u}_2''\rangle$ without resulting to any predetermined 'ideal' ν_t values and blending functions.

The effects of the dynamic forcing in reducing the thickness and impact of the artificial buffer layer, can be well interpreted by utilizing the production terms in transport equations for the resolved turbulent stresses and TKE. It is discovered that the physics underlying the formation of the artificial buffer layer is owing to the fact that the resolved $\bar{u}_{2,\mathrm{rms}}$ is excessively damped around the interface, which then results in a shift of the velocity profile to compensate the production for the resolved shear stresses.

REFERENCES

Abe, H., Kawamura, H. & Matsuo, Y. 2004 Surface heat-flux fluctuations in a turbulent channel flow up to $Re_\tau = 1020$ with $Pr = 0.025$ and 0.71. *Int. J. Heat Fluid Flow* **25**, 404–419, DNS data available from the Wall Turbulence and Heat Transfer Laboratory (Kawamura, H.) at Tokyo University of Science, http://murasun.me.noda.tus.ac.jp/turbulence/.

Baggett, J. S. 1998 On the feasibility of merging LES with RANS for the near-wall region of attached turbulent flows. In *Annu. Res. Briefs*, pp. 267–277. Center for Turbulence Research, Stanford Univ.

Batten, P., Goldberg, U. & Chakravarthy, S. 2004 Interfacing statistical turbulence closures with large-eddy simulation. *AIAA J.* **42**, 485–492.

Chapman, D. R. 1979 Computational aerodynamics development and outlook. *AIAA J.* **17**, 1293–1313.

Choi, H. & Moin, P. 1994 Effects of the computational time step on numerical solutions of turbulent flow. *J. Comp. Phys.* **113**, 1–4.

Davidson, L. 2009 Hybrid LES-RANS: back scatter from a scale-similarity model used as forcing. *Phil. Trans. R. Soc. A* **367**, 2905–2915.

Davidson, L. & Billson, M. 2006 Hybrid LES-RANS using synthesized turbulent fluctuations for forcing in the interface region. *Int. J. Heat Fluid Flow* **27**, 1028–1042.

Davidson, L. & Dahlström, S. 2005 Hybrid LES-RANS: An approach to make LES applicable at high Reynolds number. *Int. J. CFD* **19** (6), 415–427.

Davidson, L. & Peng, S. H. 2003 Hybrid LES-RANS modeling: a one-equation SGS model combined with a k-ω model for predicting recirculating flows. *Int. J. Numer. Meth. Fluids* **43**, 1003–1018.

Durbin, P. A. 1995 Separated flow computations with the k-ε-v^2 model. *AIAA J.* **33**, 659–664.

Ferziger, J. H. & Perić, M. 1999 *Computational Methods for Fluid Dynamics*, 2nd edn. Berlin: Springer.

Germano, M., Piomelli, U., Moin, P. & Cabot, W. H. 1991 A dynamic subgrid-scale eddy viscosity model. *Phys. Fluids A* **3**, 1760–1765.

Horiuti, K. 2003 Roles of non-aligned eigenvectors of strain-rate and subgrid-scale stress tensors in turbulence generation. *J. Fluid Mech.* **491**, 65–100.

Iwamoto, K., Suzuki, Y. & Kasagi, N. 2002 Reynolds number effect on wall turbulence: Toward effective feedback control. *Int. J. Heat Fluid Flow* **23**, 678–689, DNS data available from the Turbulence and Heat Transfer Laboratory (Kasagi, N.) at University of Tokyo, http://www.thtlab.t.u-tokyo.ac.jp/.

Larsson, J., Lien, F.-S. & Yee, E. 2007 The artificial buffer layer and the effect of forcing in hybrid LES/RANS. *Int. J. Heat Fluid Flow* **28**, 1443–1459.

Lilly, D. K. 1992 A proposed modification of the germano subgrid-scale closure method. *Phys. Fluids A* **4**, 633–635.

Mason, P. J. & Thomson, D. J. 1992 Stochastic backscatter in large-eddy simulations of boundary layers. *J. Fluid Mech.* **242**, 51–78.

Nikitin, N. V., Nicoud, F., Wasistho, B., Squires, K. D. & Spalart, P. R. 2000 An approach to wall modeling in large-eddy simulations. *Phys. Fluids* **12** (7), 1629–1632.

Piomelli, U., Balaras, E., Pasinato, H., Squires, K. D. & Spalart, P. R. 2003 The inner-outer layer interface in large-eddy simulations with wall-layer models. *Int. J. Heat Fluid Flow* **24**, 538–550.

Smagorinsky, J. 1963 General circulation experiments with the primitive equations, I. the basic experiment. *Mon. Weath. Rev.* **91**, 99–165.

Spalart, P. R., Jou, W. H., Strelets, M. & Allmaras, S. R. 1997 Comments on the feasibility of LES for wings, and on a hybrid RANS/LES approach. In *First AFOSR International Conference on DNS/LES* (ed. C. Liu & Z. Liu). Ruston, LA.

Temmerman, L., Hadžiabdić, M., Leschziner, M. A. & Hanjalić, K. 2005 A hybrid two-layer URANS-LES approach for large eddy simulation at high Reynolds numbers. *Int. J. Heat Fluid Flow* **26**, 173–190.

Tucker, P. G. & Davidson, L. 2004 Zonal k-l based large-eddy simulations. *Comput. Fluids* **33**, 267–287.

Wang, B.-C. & Bergstrom, D. J. 2005 A dynamic nonlinear subgrid-scale stress model. *Phys. Fluids* **17(035109)**, 1–15.

Xun, Q.-Q., Wang, B.-C. & Eugene, Y. 2011 Large-eddy simulation of turbulent heat convection in a spanwise rotating channel flow. *Int. J. Heat Mass Trans.* **54**, 698–716.